Chemistry–A European Journal
Full Paper
doi.org/10.1002/chem.202101163
Chemistry Europe
European Chemical Societies Publishing

Artificial Supramolecular Pumps Powered by Light

Stefano Corra[+],[a, b] Lorenzo Casimiro[+],[a, c, d] Massimo Baroncini,[a, e] Jessica Groppi,[a] Marcello La Rosa,[a, e] Marina Tranfić Bakić,[a, b] Serena Silvi,[a, c] and Alberto Credi*[a, b]

Dedicated to Professor Vincenzo Balzani on the occasion of his 85th birthday

Abstract: The development of artificial nanoscale motors that can use energy from a source to perform tasks requires systems capable of performing directionally controlled molecular movements and operating away from chemical equilibrium. Here, the design, synthesis and properties of pseudorotaxanes are described, in which a photon input triggers the unidirectional motion of a macrocyclic ring with respect to a non-symmetric molecular axle. The photoinduced energy ratcheting at the basis of the pumping mechanism is validated by measuring the relevant thermodynamic and kinetic parameters. Owing to the photochemical behavior of the azobenzene moiety embedded in the axle, the pump can repeat its operation cycle autonomously under continuous illumination. NMR spectroscopy was used to observe the dissipative non-equilibrium state generated in situ by light irradiation. We also show that fine changes in the axle structure lead to an improvement in the performance of the motor. Such results highlight the modularity and versatility of this minimalist pump design, which provides facile access to dynamic systems that operate under photoinduced non-equilibrium regimes.

Introduction

The realization of artificial machines and motors of molecular size is one of the most significant achievements of chemistry in the past three decades.[1,2] The utilization of these nanoscale devices in technology and medicine is a hot topic in current research.[3] A particularly stimulating challenge is the use of synthetic molecular machines to transport substrates in a controlled fashion[4] over long distances or across membranes,[5] similarly to what happens for biomolecular motors[6] such as kinesin and bacteriorhodopsin.

In living organisms, molecular and ionic species are transported passively (i.e., relying on concentration differences) across membranes by channels, whereas active transport (i.e., vectorial transfer without or against a concentration gradient) is performed by pumps. The latter devices are tasked with essential functions for the life of organisms, such as regulation and balance of substance levels, signal transduction, and energy conversion and storage.

The construction of artificial molecular pumps[7] has proven to be very challenging, as witnessed by the fact that until now only a handful of examples have been described in the literature.[8–10] All of them consist of (pseudo)rotaxanes in which the macrocyclic (ring) and the acyclic (axle) components exhibit relative unidirectional threading-dethreading motion upon application of an external stimulus.

We previously described a pseudorotaxane complex that behaves as an autonomous molecular pump powered by light.[8] The device is based on the reversible *E*–*Z* photoisomerization of azobenzene and it operates in solution at ambient temperature under continuous irradiation. The photoinduced unidirectional transit of the ring with respect to the axle was demonstrated from the determination and analysis of the thermodynamic and kinetic parameters for threading and dethreading in the *E* and *Z* configurations. Moreover, luminescence spectroscopy experiments were employed to show that under light irradiation the concentration of the uncomplexed ring evolves towards a value that is not compatible with an equilibrium state of the self-assembly processes. These experiments proved that the

[a] Dr. S. Corra,[+] Dr. L. Casimiro,[+] Prof. M. Baroncini, Dr. J. Groppi, Dr. M. La Rosa, Dr. M. Tranfić Bakić, Prof. S. Silvi, Prof. A. Credi
CLAN-Center for Light Activated Nanostructures, Istituto ISOF-CNR
Via Gobetti 101, 40129 Bologna, Italy
E-mail: alberto.credi@unibo.it

[b] Dr. S. Corra,[+] Dr. M. Tranfić Bakić, Prof. A. Credi
Dipartimento di Chimica Industriale "Toso Montanari"
Università di Bologna
Viale del Risorgimento 4, 40136 Bologna, Italy

[c] Dr. L. Casimiro,[+] Prof. S. Silvi
Dipartimento di Chimica "G. Ciamician"
Università di Bologna
Via Selmi 2, 40126 Bologna, Italy

[d] Dr. L. Casimiro[+]
Université Paris-Saclay, CNRS, PPSM
4 Avenue des Sciences, 91190 Gif-sur-Yvette, France

[e] Prof. M. Baroncini, Dr. M. La Rosa
Dipartimento di Scienze e Tecnologie Agro-alimentari
Università di Bologna
Viale Fanin 44, 40127 Bologna, Italy

[+] These authors contributed equally to this work.

Supporting information for this article is available on the WWW under https://doi.org/10.1002/chem.202101163

This manuscript is part of a special collection dedicated to Vincenzo Balzani on the occasion of his 85th birthday.

repeated photoinduced (that is, autonomous) *E*–*Z* switching leads to a stationary non-equilibrium state.[8a]

The system, however, is not very efficient and its operation was demonstrated only in dichloromethane – a solvent that maximizes the association between the ring and the axle. Here we describe the results of our efforts to (i) enhance the performance of the pump by modifying the design of the axle component, and (ii) improve the analytical tools employed to observe the operation of the system, with particular reference to its behaviour away from equilibrium.

Results and Discussion

Design of the molecular pumps

The investigated molecular pumps are based on [2]pseudorotaxane complexes formed between the dibenzo[24]crown-8 ring **1** and the molecular axles **2a**–**c** (Figure 1). The latter consist of a secondary ammonium moiety as a recognition site for the ring,[11] positioned between a photoswitchable azobenzene gate and a non-photoactive cyclopentyl pseudostopper. The previously studied molecular pump[8a,c] comprised axle **2a** and 2,3-dinaphtho[24]crown-8, whose fluorescent naphthalene moieties were instrumental in the determination of the ring concentration. In the present study we do not rely on luminescence measurements; thus, we employed dibenzo[24]crown-8, which has a cavity of the same size as that of the previously used dinaphtho crown ether and is commercially available. In the new axles **2b** and **2c**, the methylammonium substituent is linked respectively in *meta* and *ortho* to the phenyldiazene substituent on the central phenyl moiety, whereas in **2a** the connection is in *para* position.

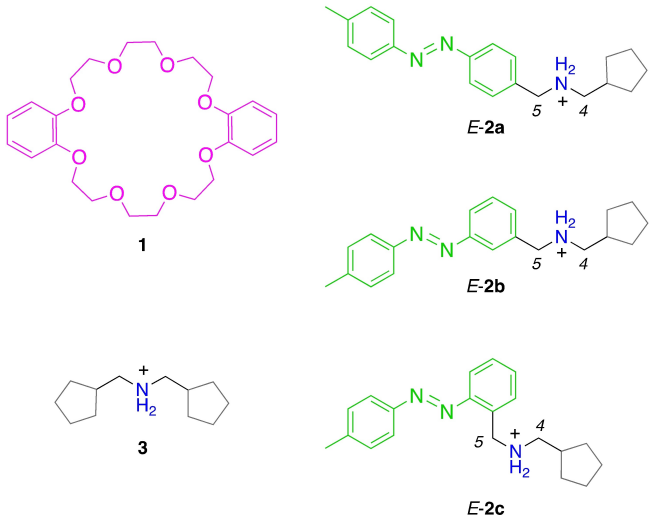

Figure 1. Structural formulas of dibenzo[24]crown-8 **1**, molecular axles **2a**-**c**, and symmetric model **3**. The numbers indicate the positions of the protons diagnostic for the formation of the pseudorotaxane in the ^{1}H NMR spectrum.

Earlier investigations showed that the *E*→*Z* photoisomerization of the azobenzene unit has two effects on the self-assembly of crown ether **1** with azobenzene-ammonium axles: (i) decrease the stability of the pseudorotaxane, and (ii) slow down the ring slipping/deslipping over the azobenzene extremity of the axle.[12] By a judicious choice of the other terminal unit of the axle, one can ensure that the threading barrier at the pseudostopper end is intermediate between those at the *E*- and *Z*-azobenzene ends, thus enabling light-induced unidirectional threading and dethreading according to a flashing energy ratchet mechanism (Figure 2). A cyclopentyl end group was found to fulfil this requirement and was therefore used as a pseudostopper in **2a**.[13] It is important to emphasize that the photoisomerization reaction causes *both* the thermodynamic (energy minima) *and* kinetic (maxima) changes necessary to implement the flashing ratchet.[14]

Another significant feature of the system is its ability to repeat threading-dethreading cycles in an autonomous fashion – that is, with a continuous energy supply under constant experimental conditions. The vast majority of artificial molecular machines reported until now are not autonomous because their operation relies on operator-modulated inputs (e.g., alternated or coordinated additions of reactants, light-dark periods, electrical potential sweeps).[1–4] For the pumps considered here, autonomous operation stems from the fact that both *E* and *Z* azobenzene isomers are photoreactive and exhibit overlapping absorption spectra, so that light of the same wavelength can trigger both the *E*→*Z* and *Z*→*E* isomerization.

The ability of the molecular pump to process light energy autonomously is a key requirement to operate in a non-equilibrium steady state.[15] As shown in Figure 3, the system is described by a cycle consisting of chemical reactions (pseudorotaxane self-assembly, horizontal processes) and photochemical reactions (*E*–*Z* isomerization, vertical processes), where only the former ones must satisfy microscopic reversibility. Under light irradiation, the concentrations of the five species are affected by the photoreactions and will not normally coincide with

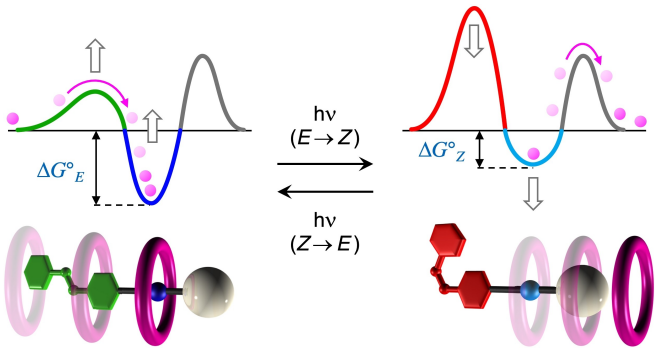

Figure 2. Simplified diagram of the free energy change as a function of the distance between the ring and axle centroids for the *E* (left) and *Z* (right) isomers of the axle. The light-triggered switching between the two profiles affords the flashing energy ratchet mechanism at the basis of unidirectional threading-dethreading. ΔG°_E and ΔG°_Z are the free energy changes associated with the assembly of either isomer of the axle with the macrocycle.

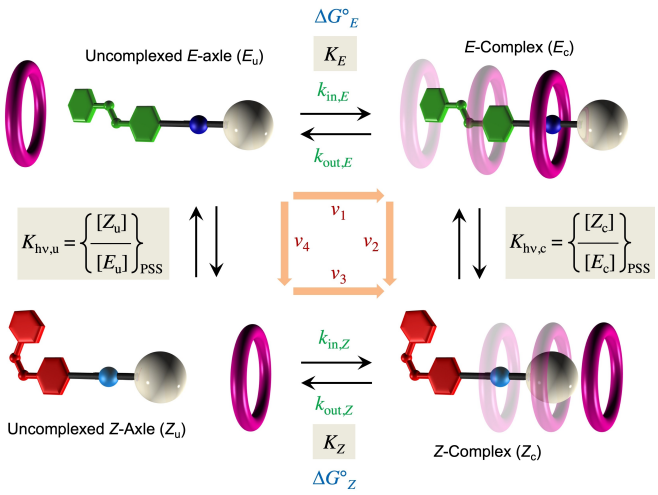

Figure 3. Cyclic reaction network representing the light-fueled operation of the pump. Horizontal and vertical processes are the self-assembly and photoisomerization reactions, respectively; the equilibrium constants and the free energy changes are referred to the reactions read from left to right and from top to bottom. The $Z \rightarrow E$ thermal isomerization steps are not indicated.

equilibrium values for the chemical reactions. Specifically, in the case of **2a** we showed that the photostationary state (PSS) for 365 nm irradiation has the same composition for the uncomplexed and complexed axle (i.e., $K_{hv,u} = K_{hv,c}$); as the *E* complex is more stable than the *Z* complex ($K_E > K_Z$), detailed balance cannot be fulfilled and the cycle is travelled clockwise. In other words, the self-assembly reactions evolve towards equilibrium without eventually reaching it, because the continuous input of photons keeps concentrations changing. At the photochemical steady state, the net rates of the individual processes are equal but non-zero ($v_{cycle} = v_1 = v_2 = -v_3 = -v_4 \neq 0$); in contrast, in a closed reaction network at thermal equilibrium the cycling rate *and* the individual rates are all zero because of detailed balance.[16]

It is worth to point out that molecular pumps of this kind exhibit directionality under two fundamentally distinct aspects, which are both essential for their molecular motor behaviour. The first one is the unidirectional nature of the relative movements of the molecular components, determined by the flashing ratchet mechanism (Figure 2); owing to this feature, threading and dethreading are not the microscopic reverse of each other, making the system a motor and not a simple switch (see ref. [2]] for a detailed discussion on this point). The second element is the directionality of the reaction cycle, that is, the fact that the cycle is travelled preferentially (i.e., faster) along the clockwise (or anticlockwise) direction. This feature, which is a clear indication of the non-equilibrium behaviour, arises from the balance-breaking photochemical processes. As pointed out earlier, for **1** and **2a** illuminated at 365 nm, the cycling direction is dictated by K_E being larger than K_Z (Figure 3).[17]

A better cycle directionality corresponds to a larger net rate at the photostationary state, which in turn should translate into a higher efficiency of the motor. In the present case, the cycle directionality can be improved by increasing the difference between K_E and K_Z; ideally, the *E* complex should be very stable, whereas the *Z* complex should be unstable. In terms of free energy changes, this condition corresponds to maximize $\Delta\Delta G^\circ = \Delta G^\circ_Z - \Delta G^\circ_E$ (Figures 2 and 3), a parameter that in fact determines the non-equilibrium steady state maintained by light.[16a] For **2a**, the larger stability of the *E* complex was attributed to π-stacking between the aromatic moieties of the crown ether and the planar *E*-azobenzene unit of the axle, a contribution that is absent in the *Z* form.[18] The *meta*- and *ortho*-linked phenyldiazene and ammonium moieties, as in **2b** and **2c**, respectively (Figure 1), are closer to each other than in **2a**; thus, it can be reasoned that the configuration of the azobenzene unit has a larger impact on the interaction between **1** and **2b–c**. Specifically, considering the bulkier non-planar shape of the *Z* isomer, we envisioned that on going from **2a** to **2b–c** the *Z* complex could be destabilized, whereas the effect on the *E* complex is expected to be small (increase of $\Delta\Delta G^\circ$). It is also crucial that the relative magnitude of the threading/dethreading energy barriers depicted in Figure 2 is maintained.

The new axles **2b** and **2c** were synthesized as hexafluorophosphate salts following the procedure reported for **2a**, namely, reductive amination between the corresponding nitrobenzylamine and cyclopentanecarbaldehyde, followed by reduction of the nitro group and subsequent Mill's coupling with 4-nitrosotoluene.[13] While the azobenzene moiety of **2b** maintains its efficient and reversible *E*-*Z* photoisomerization in solution, **2c** does not exhibit an efficient conversion to the *Z* isomer. This is most likely due to the $Z \rightarrow E$ thermal isomerization, which is almost four orders of magnitude faster than for **2a-b** (see the Supporting Information). The solvent chosen in the present investigation – acetonitrile – marks another important difference with respect to the previous studies, carried out in dichloromethane.[8] In such a low-polarity and weakly coordinating solvent, the stability constants are so large that in a 1:1 mixture of ring and axle, both the *E* and *Z* isomers are fully complexed even at sub-millimolar concentrations. Conversely, we envisioned that in acetonitrile the weaker association of the components could allow us to monitor by NMR spectroscopy all the species involved in the cycle.[13] This is important not only to detect differences between K_E and K_Z, but also to follow precisely the time-dependent concentration changes expected when the system moves away from (or returns to) equilibrium.

Stability of the pseudorotaxanes and threading-dethreading rate constants

The formation of [2]pseudorotaxane complexes between axles *E*-**2a** or *E*-**2b** and macrocycle **1** was first evaluated by ^{1}H NMR spectroscopy. A 1:1 mixture of **1** and *E*-**2a** in CD_3CN was prepared and the ^{1}H NMR spectrum was recorded at 298 K (Figure S3). In particular, the spectrum of the mixture displayed two multiplets at 4.75 ppm and 3.18 ppm, and a marked upfield shift of the aromatic signals of the axle. These spectral features indicate the involvement of H^5 and H^4 in hydrogen bonding

with the oxygen atoms of the macrocyclic cavity, and significant stacking interactions between the catechol units of **1** and the aromatic portion of the axle. These observations are consistent with the formation of a [2]pseudorotaxane whose threading-dethreading processes are slow in the NMR timescale, and are in full agreement with previous studies on the formation of threaded complexes between dialkylammonium-type axles and DB24C8.[11–13]

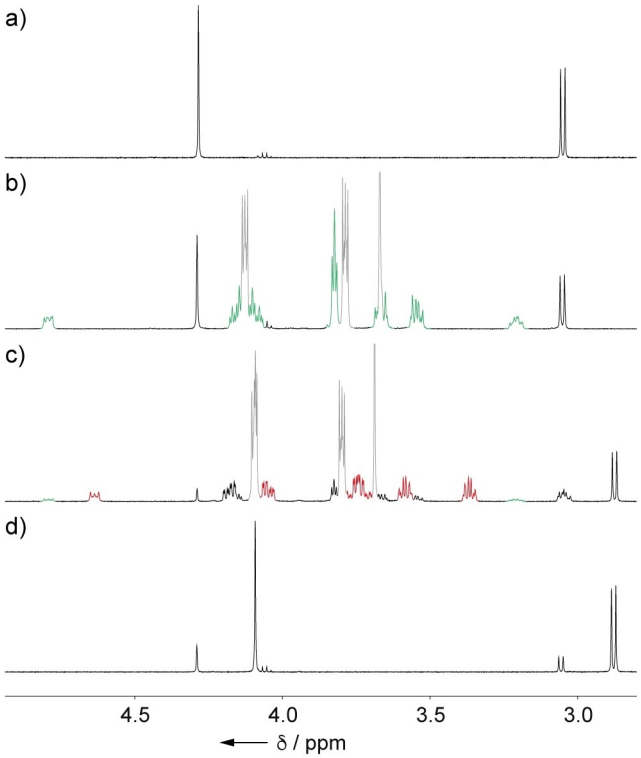

Figure 4. Partial ^{1}H NMR spectrum (500 MHz, CD_3CN, 298 K) of a) *E*-**2b**, b) 1:1 mixture of *E*-**2b** and **1** (5 mM; the signals of the *E* complex are highlighted in green), c) equilibrated 1:1 mixture of **1** and *Z*-**2b**, obtained upon exhaustive irradiation of *E*-**2b** (λ_{irr} = 365 nm, 30 min; 5 mM; the signals of the *Z* complex are highlighted in red), and d) *Z*-**2b**, obtained upon exhaustive irradiation of *E*-**2b** at 365 nm.

Table 1. Thermodynamic and kinetic data for complexation with **1** in acetonitrile at 298 K.

Axle	Isom.	K[a] [M^{-1}]	$-\Delta G^\circ$[b] [kJ mol^{-1}]	k_{in}[c] [$M^{-1}s^{-1}$]	k_{out}[c] [s^{-1}]
2a[d]	*E*	225 ± 40	13.4	22 ± 4[e]	0.1[e]
	Z	230 ± 40 200 ± 50[f]	13.5	(5.1 ± 1.0) × 10^{-2}	(2.6 ± 0.5) × 10^{-4}
2b	*E*	230 ± 30	13.5	16 ± 3[e]	0.07[e]
	Z	170 ± 30 115 ± 35 [f]	12.7	(3.1 ± 0.8) × 10^{-2}	(2.7 ± 0.5) × 10^{-4}
2c	*E*	< 50	< 10	[g]	[g]
3 [d]	–	~30[f]	~8.4	(1.3 ± 0.3) × 10^{-1}	(4.4 ± 0.9) × 10^{-3}

[a] Measured from single-point ^{1}H NMR experiments, unless noted otherwise. [b] $\Delta G^\circ = -RT \ln K$. [c] Determined from time-dependent ^{1}H NMR concentration profiles, unless noted otherwise. [d] Data from ref. [13]. [e] Determined from stopped flow UV-Vis absorption spectroscopy. [f] Calculated as k_{in}/k_{out}. [g] Not determined.

An equimolar mixture of **1** and *E*-**2b** in CD_3CN showed the same qualitative ^{1}H NMR spectral features observed in the case of *E*-**2a**, confirming the formation of a threaded complex (Figures 4 and S4). The association constant is identical within error to that determined for *E*-**2a** (Table 1), indicating that moving the phenyldiazene substituent from *para* to *meta* with respect to the dialkylammonium unit does not hamper the thermodynamic stability of the corresponding complex when the azobenzene moiety is in the *E* configuration. Conversely, the complexation of *E*-**2c** with **1** in CD_3CN is much weaker (Table 1); this observation, together with the fast $Z \rightarrow E$ back reaction, is most likely due to a [N^+–H···N] intramolecular hydrogen bonding involving the ammonium and diazene units of **2c**. Because of the low association with the crown ether (less than 20% in an equimolar mixture at 5 mM) and the poor $E \rightarrow Z$ photoconversion, axle **2c** was excluded from further investigations.

The possibility to achieve unidirectional transit of the ring along the axle (Figure 2) was examined by measuring the threading-dethreading rate constant for each isomer of axles **2a** and **2b**, and the stability constant of the complex of **1** with either axle in the *Z* form. The threading rate constant of the *E* isomers was determined from stopped flow UV-Vis absorption experiments, whereas the threading and dethreading rate constants of the *Z* isomers were measured from the fitting of the time-dependent concentration profiles observed by ^{1}H NMR after photoirradiation (see the Experimental Section and the Supporting Information for details). The ratio of the threading and dethreading rate constants was in agreement with the stability constant of the *Z* complexes. The results are summarized in Table 1.

Briefly, the threading of *E*-**2a** and *E*-**2b** with **1** is a second-order process with a rate constant (k_{in}) of 22 and 16 $M^{-1}s^{-1}$, respectively. A comparison with the data obtained for symmetric control compounds (a bis-azobenzene axle and model **3**)[12,13] shows that axle *E*-**2a** enters the macrocycle almost exclusively (> 99%) with the azobenzene extremity. Axle *E*-**2b** exhibits the same behaviour, as evidenced by its threading rate constant, which is very similar to that of *E*-**2a** and over 100 times faster than that of **3**. To determine the rate constants for the threading (k_{in}) and dethreading (k_{out}) of the *Z* complexes, *Z*-**2a** or *Z*-**2b** were first generated by irradiating a solution of the corresponding *E* isomer (λ_{irr} = 365 nm); **1** was then added and the formation of the *Z* complex was monitored by ^{1}H NMR (see the Supporting Information). The comparison with the behaviour of the model compounds – in particular, the similarity of the threading rate constants with the k_{in} value of **3** (Table 1) and the much slower value for slippage over the *Z*-azobenene moiety[12,13] – confirms that the threading and dethreading of the *Z* isomers of both **2a** and **2b** involves the cyclopentyl extremity.

These results confirm that the barriers for threading of **2a** and **2b** with **1** fulfil the order required for energy ratcheting (*E*-azobenzene < pseudostopper < *Z*-azobenzene). However, as discussed in the previous section (Figure 2), the photoinduced pumping is driven by a different stability of the *E* and *Z* complexes. In CD_3CN, the association constants of the *E* and *Z*

forms of **2a** with **1** are the same within errors; such a scenario suggests that this axle, although it exhibits the necessary kinetic asymmetry of threading, cannot behave as a light-fueled pump in combination with ring **1** in acetonitrile. Nevertheless, unidirectional transit was observed using a chemical stimulus to extrude the ring from the *Z* axle,[13] and autonomous photoinduced pumping of **2a** according to the mechanism shown in Figure 2 was demonstrated in dichloromethane using a different macrocycle.[8a]

In contrast, the stability constant of the complex of **2b** with **1** decreases from 230 to 170 M^{-1} on going from the *E* to the *Z* isomer (from 42% to 36% association in a 5 mM 1:1 mixture, see Figure S4). Although these numbers are affected by large errors, the value of K_Z determined from the ratio of the threading and dethreading rate constants ($115 \pm 35\ M^{-1}$) indicates that the drop with respect to K_E is real. The differential free energy change $\Delta\Delta G^\circ$ for the complexes of **1** with *E*- and *Z*-**2b** is around 0.8 kJ mol^{-1}, which represents a promising step forward with respect to axle **2a** whose $\Delta\Delta G^\circ$ is nearly zero.

Observation of light-induced non-equilibrium states

In order to monitor the photoinduced concentration changes after or during irradiation, we adapted an experimental setup described by Gschwind and coworkers,[19] and employed an optical fiber to deliver near UV light ($\lambda_{irr} = 369 \pm 10$ nm) from a LED source to the solution contained in the NMR probe.[20]

In a typical experiment, an equimolar mixture (10 mM) of **1** and *E*-**2a** or *E*-**2b** in CD_3CN was equilibrated in the dark, and the concentration of all the species was determined by ^{1}H NMR. At this point, the *E*→*Z* photoisomerization of the azobenzene unit of the axle was performed in situ. Under the employed conditions, irradiation afforded a PSS with a constant [*Z*]/[*E*] ratio (ca. 80%) in about 5 min (orange bars in Figure 5). Within such a short time, the disassembly of the *Z* complex is negligible, as confirmed by the fact that the concentrations of complexed and uncomplexed axle (irrespective of the configuration) are unchanged within error. Thus, the system goes out of equilibrium because the concentration of the complexed axle, which was originally an equilibrium value for the *E* isomer, it is no longer such for the *Z*-configured one. After the PSS has been reached (instantaneously, on the time scale of *Z* complex dethreading), the experiment can proceed in two distinct ways, each one leading to a fundamentally different outcome.

In a first instance, the irradiation was turned off and NMR spectra were acquired over time in the dark for 12 h. A decrease of about 5% and 20% was observed in the concentration of complexed *Z*-**2a** and *Z*-**2b**, respectively (Figure 5a), accompanied by a corresponding increase in the concentration of the uncomplexed *Z* axles. The concentrations of the *E* species – complexed and uncomplexed – exhibit a very slow increase owing to thermal *Z*→*E* isomerization. This effect is too small to be appreciated on the time scale of Figure 5; however, it can be cleanly deconvoluted from the dethreading kinetics of the *Z* complex as the two processes occur on significantly different timescales. In fact, all the reactions in the network shown in Figure 3 are at least two orders of magnitude faster than the thermal *Z*→*E* isomerization of the complexed or uncomplexed axle (see Table S1).

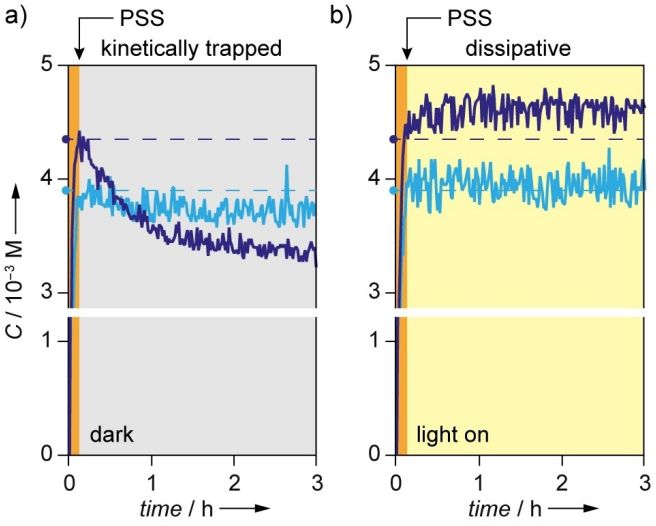

Figure 5. Time-dependent concentration profiles, determined by ^{1}H NMR, of complexed *Z*-**2a** (cyan) and complexed *Z*-**2b** (blue) quickly generated by 369 nm irradiation of an equilibrated mixture of the corresponding *E* axles and ring **1**. (a) Evolution of the kinetically trapped state in the dark. (b) Generation of a dissipative non-equilibrium state upon continuous irradiation. The orange bars mark the irradiation at high intensity to reach the PSS; the dashed lines indicate the corresponding concentration of the kinetically trapped *Z* complexes. Conditions: CD_3CN, 298 K, [**1**] = [**2a**–**b**] = 10 mM.

The changes in Figure 5a show unequivocally that the *Z* complex is less stable than the *E* one, a finding that is consistent with the different values of K_E and K_Z determined by single-point measurements in the case of **2b** (see Table 1 and related discussion). Interestingly, the small but tangible decrease in the concentration of complexed *Z*-**2a** (Figure 5a, cyan trace, and Figure S10) indicates that also for this compound $K_Z < K_E$, a difference that could not be highlighted in individual measurements of the stability constants.

It should be remarked that this experiment affords a kinetically trapped state in which the *Z* complex is photogenerated in a non-equilibrium concentration. The system evolves by dethreading of the *Z* complex on the time scale of a few hours, to reach the free energy minimum for the self-assembly reactions in the presence of the *Z* species. This new state, however, does not correspond to thermodynamic equilibrium, because the amount of *Z* and *E* isomers is determined by the photoreaction and does not follow a Boltzmann distribution. In fact, the system continues its transformation on a time scale of days by thermal *Z*→*E* isomerization, necessarily accompanied by the adjustment of the self-assembly reactions to keep up with the changing composition of the solution, until the *global* free energy minimum is reached (100% *E* isomers).

In a second instance, after the fast achievement of the PSS, the irradiation was continued with a lower intensity (about 40% of the initial value) while recording ^{1}H NMR spectra. The photon flow was attenuated to a value sufficient to maintain the PSS

composition, in order to minimize heating and photodecomposition issues. Remarkably, not only the concentration of the complexed form of both *Z* axles did not decrease, as it would be expected if the self-assembly attempted to equilibrate with the *Z* isomers, but it increased – very slightly for **2a**, in an evident manner for **2b** – above the kinetically trapped value (dashed lines in Figure 5) until a constant value was reached after ca. 1 h. Such a degree of complexation of the *Z* axle is incompatible with any equilibrium condition of the macrocycle-axle mixture and persists as long as the solution is illuminated. Once the light was switched off, the system entered the kinetically trapped regime and started to relax as shown in Figure 5a.

These observations indicate that in CD_3CN under irradiation, both **2a** and **2b** in combination with **1** reach a stationary non-equilibrium state in which light energy is continuously dissipated. Stationary states away from equilibrium resemble equilibrium states because they are time-invariant; however, as discussed above (Figure 3), in the former ones a flow continues to occur ($v_{cycle} \neq 0$). In the present case, this difference can be evidenced by analyzing the time-dependent change of the threading net rate of the *Z* axle with and without light irradiation (Figure 6). This parameter (v_3 in Figure 3) can be determined from the experimentally determined values of rate constants and concentrations according to Equation (1):

$$v_3(t) = k_{in,Z}\, C_{Z\text{-axle}}(t)\, C_{ring}(t) - k_{out,Z}\, C_{Z\text{-complex}}(t) \quad (1)$$

As shown in Figure 6a for **2b**, the threading rate upon dark relaxation of the kinetically trapped state is initially negative (i.e., the *Z* complex, photogenerated in a non-equilibrium concentration, undergoes disassembly) and subsequently decays to zero when the self-assembly processes reach equilibrium for the *E/Z* ratio dictated by the previous irradiation. Conversely, if the light source is kept on, the magnitude of the threading rate does not decay over time, but it initially increases until it reaches a constant value that is maintained throughout the irradiation (Figure 6b). The negative value of v_3 in the dissipative stationary state confirms that clockwise cycling along the network shown in Figure 3 is taking place.

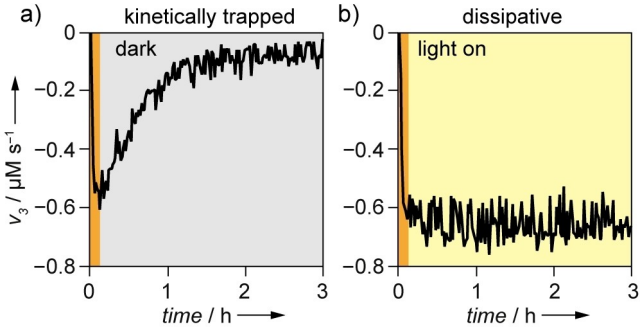

Figure 6. Threading rate of **1** and *Z*-**2b** as a function of time, calculated with equation 1 from experimentally determined rate constants (Table 1) and concentrations (Figure 5), in the dark (a) and under continued irradiation at 369 nm (b). In both cases, an equilibrated mixture of **1** and *E*-**2b** was rapidly brought to the photostationary state upon 369-nm irradiation. Conditions: CD_3CN, 298 K, [**1**] = [**2b**] = 10 mM.

From a qualitative viewpoint, a distinctive feature of the dissipative regime afforded by photochemical cycling in the present system is the over-accumulation of the *Z* complex (Figure 5b). In fact, although this species is less stable than the *E* complex, its disassembly (by slippage of the ring on the cyclopentyl end) is very slow, making this step a kinetic bottleneck for the cycle. Thus, as the system travels along the cycle by absorption of light, the concentrations of all the species involved shift progressively away from equilibrium (or kinetically trapped non-equilibrium) values, until a stationary state characterized by a uniform rate for all the branches of the network (Figure 3) is afforded. Under this condition, the molecular motor performs light-powered autonomous threading-dethreading movements that, owing to energy ratcheting (Figure 2), take place unidirectionally.

Conclusion

We have investigated the self-assembly of photoactive oriented molecular axles with dibenzo[24]crown-8 in acetonitrile. The experimentally determined stability and rate constants highlight the kinetic asymmetry of the threading-dethreading reactions and its light-induced modulation, which form the basis of an energy ratchet mechanism. As a result, these systems behave as photochemically driven supramolecular pumps wherein the ring and the axle move unidirectionally relatively to one another in response to light stimulation. Owing to the properties of azobenzene employed as a molecular photoswitch in the axle components,[21] the pumps can process light energy autonomously and can run repeatedly along their working cycle under irradiation at constant wavelength and intensity. Under this condition, a photostationary dissipative state is reached in which the light energy is employed to keep the self-assembly reactions away from thermodynamic equilibrium.

Changing the connection geometry between the azobenzene and the ammonium recognition site in the molecular axles affects substantially their behaviour: the *meta* derivative **2b** is more efficient in the molecular pumping mechanism than the previously reported *para* axle **2a**.[8,13] Conversely, the *ortho* derivative **2c** is not interesting in the present context because it exhibits a poor association with the macrocycle. Key for the improved pumping efficiency of **2b** with respect to **2a** is the larger stability difference between the *E* and *Z* complexes in the former case.

By combining a photoreactor with the NMR spectrometer, we succeeded for the first time to detect and investigate the photoinduced non-equilibrium dissipative regime of the molecular pumps. Indeed, such a photo NMR setup proved instrumental to detect the small concentration changes that occur in the transition from the kinetically trapped state populated by fast photoisomerization and the stationary non-equilibrium state reached upon prolonged irradiation. With this technique we have proved that **2a** and **1** behave as a molecular

pump not only in dichloromethane, as found previously,[8a] but also in acetonitrile; this observation could not be made with conventional spectroscopic experiments.[13]

The present results confirm the general value of the strategy, based on the combination of photoswitching and molecular recognition phenomena,[22] to achieve directional molecular movements. The minimalist design and the unsophisticated structure of the molecular components make our approach viable and flexible. Moreover, the pumping efficiency may be adjusted by modulation of the association of the ring with the different axle configurations upon changing environmental parameters such as solvent, temperature, and counterion. Additionally, such systems provide an outstanding playground to study the non-equilibrium behaviour of reaction networks under the action of light – an aspect that, despite its high scientific significance, has been so far scarcely investigated experimentally.

Experimental Section

Materials: All reagents and chemicals, including dibenzo[24]crown-8 **1** (Sigma-Aldrich 98%) were reagent-grade quality and used as received unless otherwise stated. Flash column chromatography was performed using Sigma-Aldrich Silica 40 (230–400 mesh size or 40–63 μm) as the stationary phase. Thin layer chromatography was performed on TLC Silica gel 60 F254 coated aluminum plates from Merck.

Synthesis: Compound *E*-**2a**·PF_6 was synthesized according to a previously reported procedure.[13] *E*-**2b**·PF_6 and *E*-**2c**·PF_6 were synthesized using the same protocol employed for *E*-**2a**·PF_6 with minor modifications. Detailed routes and analytical data are reported in the Supporting Information.

UV-Visible spectroscopy and photochemistry: Absorption spectra were recorded on a Perkin Elmer lambda 750 double beam spectrophotometer on air equilibrated CH_3CN (Romil) solutions at room temperature (ca. 298 K), with concentrations ranging from 10^{-5} to 10^{-3} M. Solutions were examined in quartz cells with 1.0 cm optical path length. The experimental error on the wavelength values was ±1 nm. Irradiation experiments were performed on air-equilibrated solutions, thoroughly stirred, at room temperature. A Hg medium pressure lamp (Hanau Q400, 150 W) was used; the desired irradiation wavelength was selected using an appropriate interference filter. The incident photon flow was measured by ferrioxalate actinometry in its micro version.[23] The photoisomerization quantum yields were calculated through fitting of the absorbance values over time with the photokinetic equation, using the software Berkeley Madonna 10. The absorbance values at the irradiation wavelength were fitted to compute the fraction of absorbed light and the concentrations. Another set of absorbances, at a wavelength with a larger variation, was added to the fit to minimize the error. The experimental error on the quantum yield values was estimated to be ±10%.

NMR spectroscopy and photochemistry: NMR spectra were recorded on an Agilent DD2 spectrometer operating at 500 MHz. Chemical shifts are quoted in parts per million (ppm) relative to tetramethylsilane using the residual solvent peak as a reference standard and all coupling constants (*J*) are expressed in Hertz (Hz). Photochemical reactions were performed in air-equilibrated CD_3CN solutions at 298 K inside the NMR tube, using a Led Engin LZ1-00UV00 LED illuminator (1.2 W, λ_{max} = 365 nm, FWHM = 10.22 nm) or into the spectrometer probehead, using a Prizmatix UHP-T-365-SR LED Illuminator (1.5 W, λ_{max} = 369 nm, FWHM = 15.56 nm) equipped with an FCA-SMA adaptor for optical fiber. Polymethylmetacrylate (PMMA) optical fibers (core 1500 μm, 5 m) equipped with a SMA connector on one end were purchased from Thorlabs. The other end of the optical fiber was scraped to remove the protective coating and submerged into the solution within the NMR tube to be irradiated (the fiber was contained in a glass casing to prevent contact with the solvent).

Determination of stability and rate constants: The stability constants (K_E and K_Z) were obtained from the ^{1}H NMR spectra of equimolar solutions (ca. 10^{-2} M) of the ring and the axle at 298 K using the single-point method.[24] The concentration of all the species at equilibrium was determined using the initial concentrations and the integration of the resonances of the complexed and uncomplexed species. The stability constant was calculated as K = [complex]/[ring][axle]. The threading rate constants (k_{in}) were obtained from the fitting of the time-dependent concentration profiles recorded by ^{1}H NMR upon mixing the ring and the axle components in acetonitrile at 298 K. As the threading of *E*-**2a** and *E*-**2b** is too fast to be monitored by NMR spectroscopy, the corresponding rate constants were measured by stopped flow UV-visible absorption spectroscopy, using an Applied Photophysics SX 18-MV apparatus (mixing time < 2 ms with a driving pressure of 8.5 bar). In all cases the experimental data were fitted using a mixed order kinetic model (second order for threading, first order for dethreading) using SPECFIT or Berkeley Madonna 10 software. The dethreading rate constant was obtained from the fitting by imposing $k_{in}/k_{out} = K$. The values reported in Table 1 are the average of at least three independent experiments; the error range is twice the standard deviation. The uncertainty on K_Z values calculated as k_{in}/k_{out} in Table 1 was determined from the propagation of the errors on the rate constants.

Other instruments and methods: High resolution mass spectrometry (HRMS) measurements were performed on a Waters Xevo G2-XS instrument equipped with an ESI source and a Q-TOF ion analyzer.

Acknowledgements

Financial support from the EU (H2020 ERC AdG 692981) and the Ministero dell'Università e della Ricerca (PRIN 20173L7W8K and 201732PY3X, FARE R16S9XXKX3) is gratefully acknowledged.

Conflict of Interest

The authors declare no conflict of interest.

Keywords: azobenzene · molecular machine · non-equilibrium process · photochemistry · rotaxanes

[1] a) V. Balzani, A. Credi, M. Venturi, *Molecular Devices and Machines: Concepts and Perspectives for the Nanoworld*, Wiley-VCH, Weinheim, **2008**; b) J. Wang, *Nanomachines: Fundamentals and Applications*, Wiley-VCH, Weinheim, **2013**; c) C. J. Bruns, J. F. Stoddart, *The Nature of the Mechanical Bond: From Molecules to Machines*, Wiley, Hoboken, **2017**.

[2] a) S. Erbas-Cakmak, D. A. Leigh, C. T. McTernan, A. L. Nussbaumer, *Chem. Rev.* **2015**, *115*, 10081–10206; b) S. Kassem, T. van Leeuwen, A. S. Lubbe, M. R. Wilson, B. L. Feringa, D. A. Leigh, *Chem. Soc. Rev.* **2017**, *46*, 2592–2621; c) C. Pezzato, C. Cheng, J. F. Stoddart, R. D. Astumian, *Chem. Soc. Rev.* **2017**, *46*, 5491–5507; d) M. Baroncini, L. Casimiro, C. de Vet, J. Groppi, S. Silvi, A. Credi, *ChemistryOpen* **2018**, *7*, 169–179; e) M. Baroncini, S. Silvi, A. Credi, *Chem. Rev.* **2020**, *120*, 200–268.

[3] a) P. Martinez-Bulit, A. J. Stirk, S. J. Loeb, *Trends Chem.* **2019**, *1*, 588–600; b) I. Aprahamian, *ACS Cent. Sci.* **2020**, *6*, 347–358; c) S. Corra, M. Curcio, M. Baroncini, S. Silvi, A. Credi, *Adv. Mater.* **2020**, *32*, 1906064; d) Q. Zhang, D.-H. Qu, H. Tian, B. L. Feringa, *Matter* **2020**, *3*, 355–370; e) D. Dattler, G. Fuks, J. Heiser, E. Moulin, A. Perrot, X. Yao, N. Giuseppone, *Chem. Rev.* **2020**, *120*, 310–433.
[4] a) S. Kassem, A. T. L. Lee, D. A. Leigh, A. Markevicius, J. Sola, *Nat. Chem.* **2016**, *8*, 138–143; b) C. Schaefer, G. Ragazzon, B. Colasson, M. La Rosa, S. Silvi, A. Credi, *ChemistryOpen* **2016**, *5*, 120–124; c) S. Kassem, A. T. L. Lee, D. A. Leigh, A. Markevicius, D. J. Tetlow, N. Toriumi, *Chem. Sci.* **2021**, *12*, 2065–2070.
[5] a) M. A. Watson, S. L. Cockroft, *Angew. Chem. Int. Ed.* **2016**, *55*, 1345–1349; *Angew. Chem.* **2016**, *128*, 1367–1371; b) S. Chen, Y. Wang, T. Nie, C. Bao, C. Wang, T. Xu, Q. Lin, D.-H. Qu, X. Gong, Y. Yang, L. Zhu, H. Tian, *J. Am. Chem. Soc.* **2018**, *140*, 17992–17998; c) A. Credi, *Angew. Chem. Int. Ed.* **2019**, *58*, 4108–4110; *Angew. Chem.* **2019**, *131*, 4152–4155.
[6] D. S. Goodsell, *The Machinery of Life.* Copernicus, New York, **2009**.
[7] Y. Qiu, Y. Feng, Q.-H. Guo, R. D. Astumian, J. F. Stoddart, *Chem* **2020**, *6*, 1952–1977.
[8] a) G. Ragazzon, M. Baroncini, S. Silvi, M. Venturi, A. Credi, *Nat. Nanotechnol.* **2015**, *10*, 70–75; b) L Casimiro, J. Groppi, M. Baroncini, M. La Rosa, A. Credi, S. Silvi, *Photochem. Photobiol. Sci.* **2018**, *17*, 734–740; c) A. Sabatino, E. Penocchio, G. Ragazzon, A. Credi, D. Frezzato, *Angew. Chem. Int. Ed.* **2019**, *58*, 14341–14348; *Angew. Chem.* **2019**, *131*, 14479–14486.
[9] a) C. Cheng, P. R. McGonigal, S. T. Schneebeli, H. Li, N. A. Vermeulen, C. Ke, J. F. Stoddart, *Nat. Nanotechnol.* **2015**, *10*, 547–553; b) C. Pezzato, M. T. Nguyen, D. J. Kim, O. Anamimoghadam, L. Mosca, J. F. Stoddart, *Angew. Chem. Int. Ed.* **2018**, *57*, 9325–9329; *Angew. Chem. Int. Ed.* **2018**, *130*, 9469–9473; c) Y. Qiu, B. Song, C. Pezzato, D. Shen, W. Liu, L. Zhang, Y. Feng, Q.-H. Guo, K. Cai, W. Li, H. Chen, M. T. Nguyen, Y. Shi, C. Cheng, R. D. Astumian, X. Li, J. F. Stoddart, *Science* **2020**, *368*, 1247–1253.
[10] S. Erbas-Cakmak, S. D. P. Fielden, U. Karaca, D. A. Leigh, C. T. McTernan, D. J. Tetlow, M. R. Wilson, *Science* **2017**, *358*, 340–343.
[11] a) P. R. Ashton, P. J. Campbell, E. J. T. Chrystal, P. T. Glink, S. Menzer, D. Philp, N. Spencer, J. F. Stoddart, P. A. Tasker, D. J. Williams, *Angew. Chem. Int. Ed. Engl.* **1995**, *34*, 1865–1869; *Angew. Chem.* **1995**, *107*, 1997–2001; b) P. R. Ashton, E. J. T. Chrystal, P. T. Glink, S. Menzer, C. Schiavo, N. Spencer, J. F. Stoddart, P. A. Tasker, A. J. P. White, D. J. Williams, *Chem. Eur. J.* **1996**, *2*, 709–728; c) P. R. Ashton, I. Baxter, M. C. T. Fyfe, F. M. Raymo, N. Spencer, J. F. Stoddart, A. J. P. White, D. J. Williams, *J. Am. Chem. Soc.* **1998**, *120*, 2297–2307; d) J. Groppi, L. Casimiro, M. Canton, S. Corra, M. Jafari-Nasab, G. Tabacchi, L. Cavallo, M. Baroncini, S. Silvi, E. Fois, A. Credi, *Angew. Chem. Int. Ed.* **2020**, *59*, 14825–14834; *Angew. Chem.* **2020**, *132*, 14935–14944.
[12] M. Baroncini, S. Silvi, M. Venturi, A. Credi, *Chem. Eur. J.* **2010**, *16*, 11580–11587.
[13] M. Baroncini, S. Silvi, M. Venturi, A. Credi, *Angew. Chem. Int. Ed.* **2012**, *51*, 4223–4226; *Angew. Chem. Int. Ed.* **2012**, *124*, 4299–4302.
[14] G. Ragazzon, M. Baroncini, S. Silvi, M. Venturi, A. Credi, *Beilstein J. Nanotechnol.* **2015**, *6*, 2096–2104.
[15] M. Baroncini, A. Credi, S. Silvi, in *Out-of-equilibrium Supramolecular Systems and Materials* (Eds: N. Giuseppone, A. Walther), Wiley-VCH, Weinheim, **2021**, pp. 305–336.
[16] a) R. D. Astumian, *Faraday Discuss.* **2016**, *195*, 583–597; b) M. Kathan, S. Hecht, *Chem. Soc. Rev.* **2017**, *46*, 5536–5550; c) M. Weissenfels, J. Gemen, R. Klajn, *Chem* **2021**, *7*, 23–37.
[17] A similar discussion can be made for overcrowded alkene rotary motors; see: E. M. Geertsema, S. Jan van der Molen, M. Martens, B. L. Feringa, *Proc. Natl. Acad. Sci. USA* **2009**, *106*, 16919–16924.
[18] G. Tabacchi, S. Silvi, M. Venturi, A. Credi, E. Fois, *ChemPhysChem* **2016**, *17*, 1913–1919.
[19] a) C. Feldmeier, H. Bartling, E. Riedle, R. M. Gschwind, *J. Magn. Reson.* **2013**, *232*, 39–44; b) P. Nitschke, N. Lokesh, R. M. Gschwind, *Prog. Nucl. Magn. Reson. Spectrosc.* **2019**, *114*, 86–134.
[20] For related studies on photoswitches, see: a) J. Kind, L. Kaltschnee, M. Leyendecker, C. M. Thiele, *Chem. Commun.* **2016**, *52*, 12506–12509; b) N. Mallo, P. T. Brown, H. Iranmanesh, T. S. C. MacDonald, M. J. Teusner, J. B. Harper, G. E. Ball, J. E. Beves, *Chem. Commun.* **2016**, *52*, 13576–13579; c) N. D. Dolinski, Z. A. Page, F. Eisenreich, J. Niu, S. Hecht, J. Read de Alaniz, C. J. Hawker, *ChemPhotoChem* **2017**, *1*, 125–131; d) M. M. Lerch, M. Medved, A. Lapini, A. D. Laurent, A. Iagatti, L. Bussotti, W. Szymanski, W. J. Buma, P- Foggi, M. Di Donato, B. L. Feringa, *J. Phys. Chem. A* **2018**, *122*, 955–964; e) T. J. Feuerstein, R. Muller, C. Barner-Kowollik, P. W. Roesky, *Inorg. Chem.* **2019**, *58*, 15479–15486; f) E. Stadler, S. Tassoti, P. Lentes, R. Herges, T. Glasnov, K. Zangger, G. Gescheidt, *Anal. Chem.* **2019**, *91*, 11367–11373; g) L. Cechova, J. Filo, M. Dracinsky, C. Slavov, D. Sun, Z. Janeba, T. Slanina, J. Wachtveitl, E. Prochazkova, M. Cigan, *Angew. Chem. Int. Ed.* **2020**, *59*, 15590–15594; *Angew. Chem.* **2020**, *132*, 15720–15724.
[21] S. Yu, N. D. McClenaghan, J.-L. Pozzo, *Photochem. Photobiol. Sci.* **2019**, *18*, 2102–2111.
[22] P. Tecilla, D. Bonifazi, *ChemistryOpen* **2020**, *9*, 538–553.
[23] M. Montalti, A. Credi, L. Prodi, M. T. Gandolfi, *Handbook of Photochemistry, 3rd Edition*, CRC Press, Boca Raton, **2006**.
[24] a) J. C. Andrew, C. S. Wilcox *J. Am. Chem. Soc.* **1991**, *113*, 678–680; b) K. Connors, *Binding Constants: The Measurement of Molecular Complex Stability*, Wiley-Interscience, New York, **1987**, Ch. 5, pp. 189–212.

Manuscript received: March 31, 2021
Accepted manuscript online: May 5, 2021
Version of record online: June 2, 2021

